Upper-bounded and sliced Jaynes- and anti-Jaynes-Cummings Hamiltonians and Liouvillians in cavity quantum electrodynamics

W. Rosado[1], G. D. de Moraes Neto[1], F. O. Prado[2], and M. H. Y. Moussa[1]

[1]*Instituto de Física de São Carlos, Universidade de São Paulo, Caixa Postal 369, 13560-970, São Carlos, São Paulo, Brazil and*

[2]*Universidade Federal do ABC, Rua Santa Adélia 166, Santo André, São Paulo 09210-170, Brazil*

arXiv:1410.5457v1 [quant-ph] 20 Oct 2014

In this paper, we present a protocol to engineer upper-bounded and sliced Jaynes-Cummings and anti-Jaynes-Cummings Hamiltonians in cavity quantum electrodynamics. In the upper-bounded Hamiltonians, the atom-field interaction is confined to a subspace of Fock states ranging from $|0\rangle$ up to $|4\rangle$, while in the sliced interaction the Fock subspace ranges from $|M\rangle$ up to $|M+4\rangle$. We also show how to build upper-bounded and sliced Liouvillians irrespective of engineering Hamiltonians. The upper-bounded and sliced Hamiltonians and Liouvillians can be used, among other applications, to generate steady Fock states of a cavity mode and for the implementation of a quantum-scissors device for optical state truncation.

PACS numbers: 32.80.-t, 42.50.Ct, 42.50.Dv

INTRODUCTION

The engineering of effective Hamiltonians has played an important role in quantum information theory, where the design of interactions suited to implementing quantum logical processes is a key ingredient [1–3]. Engineered interactions are also required for quantum simulation, where controllable laboratory systems are assumed to simulate quantum phenomena that share the same mathematical structure but are difficult to handle in the laboratory [4]. Moreover, engineered interactions are a precondition for the reservoir engineering technique, [5] where a target state is protected. The strategy of switching off the reservoir and thus protecting any quantum state, based on the engineering of a nonstationary quantum system —where a time-dependent Hamiltonian must be appropriately prepared— has also been advanced [6].

More recently, two schemes were presented to produce steady nonclassical states within cavity QED [7] and trapped ions [8], both relying on suitably designed interactions. In the former case, selected Jaynes-Cummings interactions are required where the two-level atom interacts with only two neighboring Fock states of the cavity mode. These effective interactions are further used for atomic reservoir engineering and steady Fock states of the radiation field are produced. In the latter case, upper-, lower-bounded and sliced Jaynes-Cummings (JC) and anti-Jaynes-Cummings (AJC) Hamiltonians are required. The upper-bounded (lower-bounded) interaction acts upon Fock subspaces ranging from $|0\rangle$ to $|M\rangle$ ($|N\rangle$ to ∞) and the sliced one is confined to a Fock subspace ranging from $|M\rangle$ to $|N\rangle$, for any $M < N$. Whereas the upper-bounded (*ub*) JC or AJC interactions are shown to drive any initial state to a quasi-steady Fock state $|N\rangle$, the sliced one is shown to produce steady superpositions of Fock states confined to the sliced subspace $\{|N\rangle, |N+1\rangle\}$.

In this contribution, we present a strategy to engineer *ub* and sliced JC and AJC Hamiltonians in cavity QED which, as already shown in the context of trapped ions [8], can be used, among other purposes, to produce steady Fock states and to implement a quantum-scissors device for optical state truncation. We stress that the technique used to engineer *ub* and sliced interactions in cavity QED is completely different from that used with trapped ions, where a suitable adjustment of the Lamb-Dicke parameter is sufficient to bring about the desired interactions. In the other hand, as should be clear below, in cavity QED the required interactions results from appropriate adjustments in a sequence of Raman-type transitions. It is worth emphasizing that our protocol can also be used in other platforms such as circuit QED with fluxonium transitions [9].

Here we focus on the engineering of *ub* Hamiltonians acting upon Fock subspaces ranging from $|0\rangle$ up to $|4\rangle$. From these Hamiltonians we show how to derive master equations with *ub* Liouvillians via the atomic reservoir engineering scheme, which are then employed to produce the steady Fock states $|2\rangle$, $|3\rangle$, and $|4\rangle$. Sliced Hamiltonians confined to Fock subspaces ranging from $|M\rangle$ up to $|M+4\rangle$ are also derived and used to generate sliced Liouvillians which produce steady superpositions of Fock states confined to the associated sliced subspaces. Moreover, we present a strategy to generate *ub* and sliced master equations without needing first to engineer *ub* and sliced Hamiltonians, which can also be used to produce steady Fock states. We advance that the present scheme can be applied to a network of dissipative oscillators to produce steady entanglements in the network corresponding to

a steady Fock state in a given normal mode [10]. Finally, we stress that the scheme used in the present manuscript, as well as that in Ref. [7], rely on a strategy to engineer selective atom-field interactions presented in Ref. [11]. Other schemes to engineer selective transtions or quantum-scissors have also been reported [12].

It would be interesting at this point to recall an early theoretical proposal to generate highly excited Fock states from an initial coherent state prepared in the vibrational degrees of freedom of a trapped ion [13]. In that scheme, the authors took only the relaxation mechanism of the electronic states into account. Differently, in our proposal, we also consider the decay of the cavity mode in which the steady Fock state is prepared; in fact, we take advantage of this inevitable decay to produce our steady states, which are achieved irrespectively of the initial state of the cavity mode. We also note that various schemes have been presented to produce steady states in cavity QED and trapped ion, other than those mentioned above [5, 7]. These protocols rely on reservoir engineering schemes [14], feedback loops [15], and quasi-local control [16]. Nonequilibrium number states up to 2 photons have long been prepared in cavity QED [17], as in most suitable platforms, such as ion traps [18], and, lately, in circuit QED [19], where number states up to 6 were achieved. More recently, a quantum feedback technique was used to produce Fock states with photon numbers up to 7 and probability around 0.4, in cavity QED [20].

UPPER-BOUNDED AND SLICED JC AND AJC INTERACTIONS

Interactions confined to the Fock subspaces $\{|0\rangle, |1\rangle, |2\rangle\}$ and $\{|M\rangle, |M+1\rangle, |M+2\rangle\}$

We start by considering the engineering of *ub* and sliced JC and AJC interactions confined to the Fock subspaces $\{|0\rangle, |1\rangle, |2\rangle\}$ and $\{|M\rangle, |M+1\rangle, |M+2\rangle\}$. To this end, we consider the atomic level configuration sketched in Fig. 1(a), where the ground and excited states g and e are coupled through Raman transitions to the auxiliary states f and h. A cavity mode ω induces the transitions $g \leftrightarrow f, h$ with strengths λ_1 and λ_2 and detunings Δ_1 and Δ_2, while a laser field ω_L induces the transitions $e \leftrightarrow f, h$ with strengths Ω_1 and Ω_2 and detunings $\tilde{\Delta}_1$ and $\tilde{\Delta}_2$. The Hamiltonian describing the system in the interaction picture reads

$$H = \lambda_1 \sigma_{fg} a \, \mathrm{e}^{-i\Delta_1 t} + \lambda_2 \sigma_{hg} a \, \mathrm{e}^{i\Delta_2 t} + \Omega_1 \sigma_{fe} \, \mathrm{e}^{-i\tilde{\Delta}_1 t} + \Omega_2 \sigma_{he} \, \mathrm{e}^{i\tilde{\Delta}_2 t} + H.c., \tag{1}$$

where $\sigma_{rs} = |r\rangle\langle s|$, r and s labelling the atomic states involved, and we define the detunings $\Delta_1 = \omega - \omega_f$, $\Delta_2 = \omega_h - \omega$, $\tilde{\Delta}_1 = \omega_L - \omega_f$, and $\tilde{\Delta}_2 = \omega_h - \omega_L$. It is straightforward to show that, under the conditions $\sqrt{\bar{n}+1}\lambda_j \ll \Delta_j$ ($\bar{n}$ being the mean excitation of the field) and $\Omega_j \ll \tilde{\Delta}_j$ ($j = 1, 2$), we derive the effective interaction ([21])

$$H_{eff} = \chi a^\dagger a \sigma_{gg} + \varpi \sigma_{ee} + \textstyle\sum_j \zeta_j \, \mathrm{e}^{i\theta_j t} \, \sigma_{ge} a^\dagger + H.c.$$

where $\chi = \lambda_1^2/\Delta_1 - \lambda_2^2/\Delta_2$ and $\zeta_j = (\lambda_j \Omega_j/2)\left(1/\Delta_j + 1/\tilde{\Delta}_j\right)$ stand for off- and on-resonant atom-field couplings, $\varpi = \Omega_1^2/\tilde{\Delta}_1 - \Omega_2^2/\tilde{\Delta}_2$ is the frequency level shift due to the action of the laser field, and $\theta_j = (-1)^{\delta_{1j}}\left(\tilde{\Delta}_j - \Delta_j\right)$ are convenient detunings required for the engineering process. The unitary transformation $U = \exp\left[-i\left(\chi a^\dagger a \sigma_{gg} + \varpi \sigma_{ee}\right) t\right]$, takes H_{eff} into the form

$$H_{eff} = \textstyle\sum_n \left(\zeta_n^{(1)} \, \mathrm{e}^{i\phi_n^{(1)} t} + \zeta_n^{(2)} \, \mathrm{e}^{i\phi_n^{(2)} t}\right) \sigma_{ge} \, |n+1\rangle\langle n| + H.c.,$$

where $\phi_n^{(j)} = \xi_n + \theta_j$ and $\zeta_n^{(j)} = \sqrt{n+1}\zeta_j$, with $\xi_n = (n+1)\,\chi - \varpi$. Finally, writing the Hamiltonian in the form

$$\begin{aligned} -H_{eff} = {} & \zeta_1 \, \mathrm{e}^{i\phi_0^{(1)} t}\left(|1\rangle\langle 0| + \sqrt{2}\,|2\rangle\langle 1| \, \mathrm{e}^{i\left(\phi_1^{(1)} - \phi_0^{(1)}\right)t} + ...\right)\sigma_{ge} \\ & + \zeta_2 \, \mathrm{e}^{i\phi_1^{(2)} t}\left(|1\rangle\langle 0| \, \mathrm{e}^{i\left(\phi_0^{(2)} - \phi_1^{(2)}\right)t} + \sqrt{2}\,|2\rangle\langle 1| + \sqrt{3}\,|3\rangle\langle 2| \, \mathrm{e}^{i\left(\phi_2^{(2)} - \phi_1^{(2)}\right)t} + ...\right)\sigma_{ge} \end{aligned}$$

we ready find that by adjusting the parameters such that

$$\phi_0^{(1)} = \phi_1^{(2)} = 0, \tag{2a}$$

$$|\chi| \gg \sqrt{2}\,|\zeta_1|, \sqrt{3}\,|\zeta_2|, \tag{2b}$$

we obtain the *ub* Hamiltonian

$$H_{ub} = \zeta_1 \sigma_{ge} A_{ub}^\dagger + H.c., \tag{3}$$

with the field operator

$$A_{ub}^\dagger = |1\rangle\langle 0| + \left(\sqrt{2}\zeta_2/\zeta_1\right)|2\rangle\langle 1|.$$

We have thus engineered the *ub* JC Hamiltonian confined to the Fock subspace $\{|0\rangle, |1\rangle, |2\rangle\}$. To achieve a sliced JC Hamiltonian confined to the Fock subspace $\{|M\rangle, |M+1\rangle, |M+2\rangle\}$, we redefine the conditions in Eq. (2) to

$$\begin{aligned} \phi_M^{(1)} &= \phi_{M+1}^{(2)} = 0, \\ |\chi| &\gg \left|\zeta_{M+1}^{(1)}\right|, \left|\zeta_{M+2}^{(2)}\right|, \end{aligned}$$

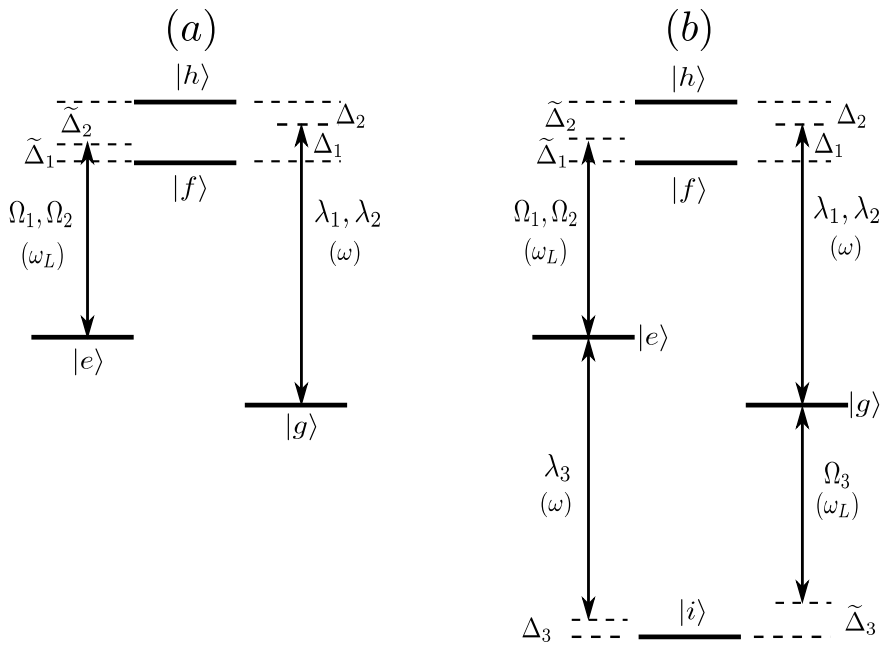

FIG. 1: (a) Four-level atomic configuration to engineer the *ub* and sliced JC Hamiltonians acting upon Fock subspaces ranging from $|0\rangle$ to $|2\rangle$ and $|M\rangle$ to $|M+2\rangle$, and (b) Five-level atomic configuration to engineer the *ub* and sliced JC Hamiltonians acting upon Fock subspaces ranging from $|0\rangle$ to $|3\rangle$ and $|M\rangle$ to $|M+3\rangle$.

leading us to the sliced Hamiltonian

$$H_s = \zeta_M^{(1)} \sigma_{ge} A_s^\dagger + H.c., \tag{4}$$

with the field operator

$$A_s^\dagger = |M+1\rangle\langle M| + \left(\zeta_{M+1}^{(2)}/\zeta_M^{(1)}\right)|M+2\rangle\langle M+1|.$$

It is worth noting that both the *ub* and sliced AJC Hamiltonians follow from the same atomic configuration in Fig. 1(a), but with the cavity mode and the laser field tuned to the reversed transitions $e \leftrightarrow f, h$ and $g \leftrightarrow f, h$, respectively. We also observe that, instead of the four-level configuration presented in Fig. 1(a), a rhombus-like level configuration can also be used to generate Hamiltonians (3) and (4). This latter configuration avoids the required proximity of levels f and h in Fig. 1, maintaining, however, all the conditions and relations exactly as derived above. Finally, we observe that the AJC interactions confined to the Fock subspaces $\{|0\rangle, |1\rangle, |2\rangle\}$ and $\{|M\rangle, |M+1\rangle, |M+2\rangle\}$ can be generated by interchanging the transitions driven by the cavity mode and the laser, tuning the quantum (classical) field to drive the transition e $(g) \leftrightarrow f, h$ instead of g $(e) \leftrightarrow f, h$.

Interactions confined to the Fock subspaces $\{|0\rangle, |1\rangle, |2\rangle, |3\rangle\}$ and $\{|M\rangle, |M+1\rangle, |M+2\rangle, |M+3\rangle\}$

To engineer the *ub* and sliced Hamiltonians confined to Fock subspaces $\{|0\rangle, |1\rangle, |2\rangle, |3\rangle\}$ and $\{|M\rangle, |M+1\rangle, |M+2\rangle, |M+3\rangle\}$, we must add another level $|i\rangle$ to the atomic configuration sketched in Fig. 1(a), as shown in Fig. 1(b). Now, the cavity mode (laser field) also induces the Raman transition $e \leftrightarrow i$ ($g \leftrightarrow i$) to the additional auxiliary state with coupling strength λ_3 (Ω_3) and detuning Δ_3 ($\tilde{\Delta}_3$). The Hamiltonian describing the system in the interaction picture reads

$$\begin{aligned} H = {} & \lambda_1 \sigma_{fg} a \, \mathrm{e}^{-i\Delta_1 t} + \lambda_2 \sigma_{hg} a \, \mathrm{e}^{i\Delta_2 t} + \lambda_3 \sigma_{hg} a \, \mathrm{e}^{i\Delta_3 t} \\ & + \Omega_1 \sigma_{fe} \, \mathrm{e}^{-i\tilde{\Delta}_1 t} + \Omega_2 \sigma_{he} \, \mathrm{e}^{i\tilde{\Delta}_2 t} + \Omega_2 \sigma_{he} \, \mathrm{e}^{i\tilde{\Delta}_3 t} + H.c., \end{aligned} \tag{5}$$

where $\Delta_3 = \omega_e + \omega_i - \omega$, $\tilde{\Delta}_3 = \omega_i - \omega_L$, and all the other parameters are those defined above. By analogy with the former reasoning used to obtain Hamiltonians (3) and (4), we next consider the conditions $\sqrt{\bar{n}+1}\lambda_j \ll \tilde{\Delta}_j$, $\Omega_j \ll \Delta_j$ ($j = 1, 2, 3$), and

$$\Phi_0^{(1)} = \Phi_1^{(2)} = \Phi_2^{(3)} = 0, \tag{6a}$$

$$|\chi - \tilde{\chi}| \gg \sqrt{2}\,|\zeta_1|, \sqrt{3}\,|\zeta_2|, 2\,|\zeta_3|, \tag{6b}$$

where $\Phi_n^{(j)} = \Xi_n + \theta_j$, $\Xi_n = \xi_n - (n+1)\,\tilde{\chi} + \Omega_3^2/\tilde{\Delta}_3$, $\tilde{\chi} = \lambda_3^2/\Delta_3$, and ξ_n, θ_j,, and ζ_j are as defined above, now with $j = 1, 2, 3$. When the auxiliary level i is disregarded, the uppercase parameters ($\Phi_n^{(j)}$,Ξ_n) recover those in lowercase ($\phi_n^{(j)}$,ξ_n) for $j = 1, 2$. Under the above conditions, we derive the *ub* Hamiltonian

$$H_{ub} = \zeta_1 \sigma_{ge} B_{ub}^{\dagger} + H.c., \tag{7}$$

with the field operator

$$A_{ub}^{\dagger} = |1\rangle\langle 0| + \left(\sqrt{2}\zeta_2/\zeta_1\right)|2\rangle\langle 1| + \left(\sqrt{3}\zeta_3/\zeta_1\right)|3\rangle\langle 2|. \tag{8}$$

Again, we achieve a sliced JC Hamiltonian confined to the Fock subspace $\{|M\rangle, |M+1\rangle, |M+2\rangle, |M+3\rangle\}$ by redefining the conditions in Eq. (6) to

$$\begin{aligned} \Phi_M^{(1)} = \Phi_{M+1}^{(2)} = \Phi_{M+2}^{(3)} = 0, \\ |\chi| \gg \left|\zeta_{M+1}^{(1)}\right|, \left|\zeta_{M+2}^{(2)}\right|, \left|\zeta_{M+3}^{(3)}\right|, \end{aligned}$$

leading us to the sliced interaction

$$H_s = \zeta_M^{(1)} \sigma_{ge} B_s^\dagger + H.c., \tag{9}$$

with the field operator

$$A_s^\dagger = |M+1\rangle\langle M| + \left(\zeta_{M+1}^{(2)}/\zeta_M^{(1)}\right)|M+2\rangle\langle M+1| + \left(\zeta_{M+2}^{(3)}/\zeta_M^{(1)}\right)|M+3\rangle\langle M+2|.$$

To generate the AJC interactions confined to the Fock subspaces $\{|0\rangle, |1\rangle, |2\rangle\}$ and $\{|M\rangle, |M+1\rangle, |M+2\rangle\}$, we have again to interchange the transitions $g, e \leftrightarrow i$ driven by the cavity mode and the laser field. Finally, we observe that, by inserting an additional auxiliary level close to i, we can obtain ub and sliced interactions confined to the Fock subspaces ranging from $|0\rangle$ to $|4\rangle$ and $|M\rangle$ to $|M+4\rangle$.

VALIDITY OF THE ENGINEERED INTERACTIONS

We next analyze the validity of the engineered ub and sliced Hamiltonians described by Eqs. 3, 4, 7, and 9. To this end, we compare numerically the sinusoidal Rabi oscillations of the cavity mode population coming from these effective interactions with those derived from the complete Hamiltonians in Eqs. 1 and 5.

Interactions confined to the Fock subspaces $\{|0\rangle, |1\rangle, |2\rangle\}$ and $\{|M\rangle, |M+1\rangle, |M+2\rangle\}$

We start by analyzing the validity of the engineered ub interaction given by Eq. (3), confined to the Fock subspaces $\{|0\rangle, |1\rangle, |2\rangle\}$. Assuming the initial state $(|0\rangle + |2\rangle) \otimes (|g\rangle + |e\rangle)/2$, in Fig. 2(a) we plot, against the interaction parameter $\zeta_1 t$, the probabilities $\mathcal{P}_0$, $\mathcal{P}_1$, and $\mathcal{P}_2$ of measuring the cavity mode in Fock states $|0\rangle$, $|1\rangle$, and $|2\rangle$. We have assumed typical coupling strengths, $\lambda_1 = \lambda_2 = 5 \times 10^5$ Hz [22], and set the detunings to $\Delta_1 = 2\Delta_2 = 10\lambda_1$ and $\theta_1 = \theta_2/2 = \lambda_1/10$, to obtain $\tilde{\Delta}_1 = 99\tilde{\Delta}_2/52 = 9.9\lambda_1$. Finally, with $\Omega_1 = 2\sqrt{2}\Omega_2 = \lambda_1/5\sqrt{2}$, we get $\zeta_1 = \sqrt{2}\zeta_2 = 1.7 \times 10^3$ Hz and, consequently, the ub operator: $A_{ub}^\dagger = |1\rangle\langle 0| + |2\rangle\langle 1|$. These parameters seem quite suitable for the derivation of the effective interaction, as confirmed by the good agreement in Fig. 2(a) between the light curves, derived from the full Hamiltonian (1), and the dark ones computed from the engineered interaction (3), given by $\mathcal{P}_0 = \mathcal{P}_2 = [1 + \cos^2(\zeta_1 t)]/4$ and $\mathcal{P}_1 = \sin^2(\zeta_1 t)/2$.

While $\mathcal{P}_0$ and $\mathcal{P}_1$ are exposed in the foreground, $\mathcal{P}_2$ is shown in the inset. The probability $\mathcal{P}_3$, which is evidently null when computed from the effective interaction, oscillates near zero for the full Hamiltonian, as shown by the dashed curve.

To analyze the validity of the engineered sliced interaction in Eq. (4), we assume $M = 3$ to confine it to the Fock subspace $\{|3\rangle, |4\rangle, |5\rangle\}$. We assume the initial state $(|3\rangle + |5\rangle) \otimes (|g\rangle + |e\rangle)/2$ to plot the probabilities $\mathcal{P}_3$, $\mathcal{P}_4$, and $\mathcal{P}_5$, in Fig. 2(b), against the interaction parameter $\zeta_3^{(1)} t$ (with $\zeta_3^{(1)} = 2\zeta_1$), of measuring the cavity mode in Fock states $|3\rangle$, $|4\rangle$, and $|5\rangle$. With typical coupling strengths, $\lambda_1 = \lambda_2 = 5 \times 10^5$ Hz, and setting $\Delta_1 = 2\Delta_2 = 20\lambda_1$ and $\theta_1 = 4\theta_2/5 = \lambda_1/5$, we obtain $\tilde{\Delta}_1 = 79.2\tilde{\Delta}_2/41 = 19.8\lambda_1$. Moreover, with laser-field strengths $\Omega_1 = \sqrt{5}\Omega_2 = \lambda_1/5\sqrt{5}$, we obtain $\zeta_1 = \sqrt{2}\zeta_2 = 6 \times 10^2$ Hz and, consequently: $A_s^\dagger = |4\rangle\langle 3| + |5\rangle\langle 4|$. Again we observe good agreement between the light curves, numerically computed from the full Hamiltonian (1), and the dark ones, analytically computed from the engineered interaction (4), given by $\mathcal{P}_3 = \mathcal{P}_5 = \left[1 + \cos^2\left(\zeta_3^{(1)} t\right)\right]/4$ and $\mathcal{P}_4 = \sin^2\left(\zeta_3^{(1)} t\right)/2$. While $\mathcal{P}_3$ and $\mathcal{P}_4$ are exposed in the foreground, $\mathcal{P}_5$ is shown in the inset. The probabilities $\mathcal{P}_2$ and $\mathcal{P}_6$, which are null for the effective interaction, oscillate near zero for the full Hamiltonian, as shown by the dashed curves in the foreground and the inset, respectively.

Interactions confined to the Fock subspaces $\{|0\rangle, |1\rangle, |2\rangle, |3\rangle\}$ and $\{|M\rangle, |M+1\rangle, |M+2\rangle, |M+3\rangle\}$

Next, analyzing the validity of the engineered *ub* interaction (7), confined to the Fock subspace $\{|0\rangle, |1\rangle, |2\rangle, |3\rangle\}$, we assume the initial state $(|1\rangle + |3\rangle) \otimes (|g\rangle + |e\rangle)/2$, so as to plot the probabilities $\mathcal{P}_0$ to $\mathcal{P}_3$ against the interaction parameter $\zeta_1 t$, in Fig. 3(a). The typical strengths, $\lambda_1 = \lambda_2 = \lambda_3 = 5 \times 10^5$ Hz, and the detunings set at $\Delta_1 = \Delta_2/2 = \Delta_3 = 10\lambda_1$ and $\theta_1 = \theta_2/2 = \theta_3/3 = \lambda_1/20$, lead to $\tilde{\Delta}_1 = 199\tilde{\Delta}_2/402 = 199\tilde{\Delta}_3/203 = 10.15\lambda_1$. Finally, with $\Omega_1 = \Omega_2/\sqrt{2} = \sqrt{3}\Omega_3 = \lambda_1/20$, we obtain $\zeta_1 = \sqrt{2}\zeta_2 = \sqrt{3}\zeta_3 = 1.77 \times 10^3$ Hz and, consequently: $A_{ub}^\dagger = |1\rangle\langle 0| + |2\rangle\langle 1| + |3\rangle\langle 2|$. As in the figures analyzed above, the light curves, derived from the full Hamiltonian, are in good agreement with the dark ones arising from the engineered interaction (7) and given by $\mathcal{P}_0 = \mathcal{P}_2/2 = \sin^2(\zeta_1 t)/4$ and $\mathcal{P}_1 = 2\mathcal{P}_3 - 1/2 = \cos^2(\zeta_1 t)/2$. While $\mathcal{P}_0$ and $\mathcal{P}_1$ are in the foreground, $\mathcal{P}_2$ and $\mathcal{P}_3$ are in the inset. The probability $\mathcal{P}_4$, which is null when computed from the effective interaction,

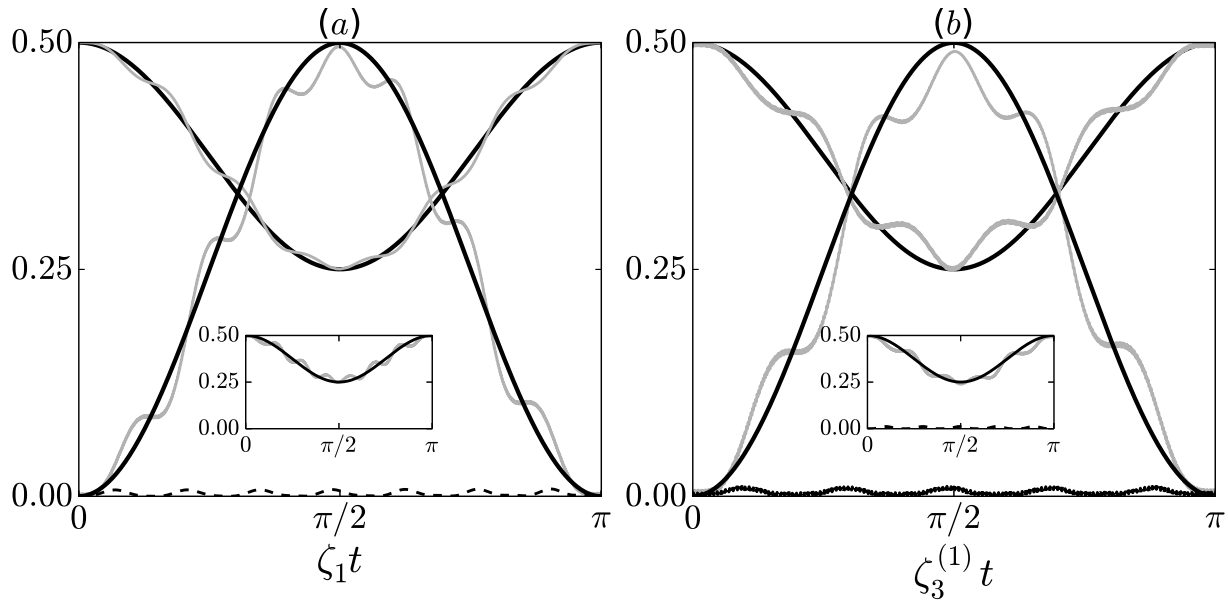

FIG. 2: (a) Probabilities $\mathcal{P}_0$ to $\mathcal{P}_3$ of measuring the cavity mode in the Fock states $|0\rangle$ to $|3\rangle$, computed from the engineered (3) and the full (1) Hamiltonians, shown by dark and light lines, respectively. $\mathcal{P}_0$ and $\mathcal{P}_1$ are exposed in the foreground while $\mathcal{P}_2$ is shown in the inset. $\mathcal{P}_3$, which is null for the effective interaction, oscillates near zero for the full Hamiltonian, as shown by the dashed curve. (b) Probabilities $\mathcal{P}_2$ to $\mathcal{P}_6$ of measuring the cavity mode in the Fock states $|3\rangle$ to $|5\rangle$, computed from the engineered (4) and the full (1) Hamiltonians, shown by dark and light lines, respectively. $\mathcal{P}_3$ and $\mathcal{P}_4$ are exposed in the foreground while $\mathcal{P}_5$ is shown in the inset. $\mathcal{P}_2$ and $\mathcal{P}_6$, which are null for the effective interaction, oscillates near zero for the full Hamiltonian as shown by the dashed curves in the foreground and the inset, respectively.

oscillates near zero for the full Hamiltonian, as shown by the dashed curve.

Regarding the validity of the engineered sliced interaction (9), we assume $M = 3$ to confine it to the Fock subspace $\{|3\rangle, |4\rangle, |5\rangle, |6\rangle\}$. Assuming the initial state $(|3\rangle + |6\rangle) \otimes (|g\rangle + |e\rangle)/2$, we plot the probabilities $\mathcal{P}_3$ to $\mathcal{P}_6$ against the interaction parameter $\zeta_3^{(1)} t$ (with $\zeta_3^{(1)} = 2\zeta_1$), in Fig. 3(b). With the typical coupling strengths, $\lambda_1 = \lambda_2 = \lambda_3 = 5 \times 10^5$ Hz and the detunings set at $\Delta_1 = \Delta_2/2 = \Delta_3 = 20\lambda_1$ and $\theta_1 = 4\theta_2/5 = 2\theta_3/3 = \lambda_1/10$, we have $\tilde{\Delta}_1 = 159.2\tilde{\Delta}_2/321 = 199\tilde{\Delta}_3/201.5 = 20.15\lambda_1$. Moreover, with the laser-field strengths $\Omega_1 = \sqrt{5}\Omega_2/4 = \sqrt{6}\Omega_3/2 = \lambda_1/20\sqrt{5}$, we have $\zeta_1 = \sqrt{5}\zeta_2/2 = \sqrt{6}\zeta_3/2 = 1.1 \times 10^3$ Hz and, consequently: $A_{ub}^{\dagger} = |4\rangle\langle 3| + |5\rangle\langle 4| + |6\rangle\langle 5|$. We observe good agreement between the light curves, computed from the full Hamiltonian, and the dark ones, calculated from

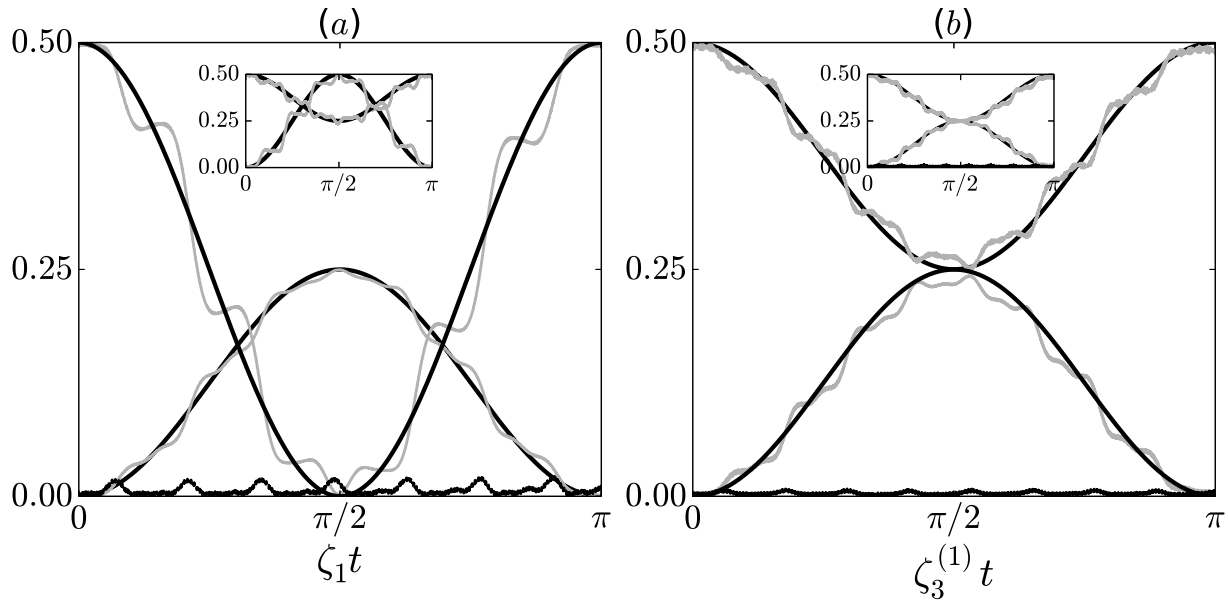

FIG. 3: (a) Probabilities $\mathcal{P}_0$ to $\mathcal{P}_4$ of measuring the cavity mode in the Fock states $|0\rangle$ to $|4\rangle$, computed from the engineered (7) and the full (1) Hamiltonians, shown by dark and light lines, respectively. $\mathcal{P}_0$ and $\mathcal{P}_1$ are exposed in the foreground while $\mathcal{P}_2$ and $\mathcal{P}_3$ are in the inset. $\mathcal{P}_4$, which is null for the effective interaction, oscillate near zero for the full Hamiltonian, as shown by the dashed curve. (b) Probabilities $\mathcal{P}_2$ to $\mathcal{P}_7$ of measuring the cavity mode in the Fock states $|2\rangle$ to $|7\rangle$, computed from the engineered (9) and the full (1) Hamiltonians, shown by dark and light lines, respectively. $\mathcal{P}_3$ and $\mathcal{P}_4$ are exposed in the foreground while $\mathcal{P}_5$ and $\mathcal{P}_6$ are in the inset. $\mathcal{P}_2$ and $\mathcal{P}_7$, which are null for the effective interaction, oscillate near zero for the full Hamiltonian, as shown by the dashed curves in the foreground and the inset, respectively.

the engineered interaction (9), given by $\mathcal{P}_3 = \mathcal{P}_6 = \left[1 + \cos^2\left(\zeta_3^{(1)} t\right)\right]/4$ and $\mathcal{P}_4 = \mathcal{P}_5 = \sin^2\left(\zeta_3^{(1)} t\right)/4$. While $\mathcal{P}_3$ and $\mathcal{P}_4$ are exposed in the foreground, $\mathcal{P}_5$ and $\mathcal{P}_6$ are shown in the inset. The probabilities $\mathcal{P}_2$ and $\mathcal{P}_7$, which are null for the effective interaction, oscillate near zero for the full Hamiltonian, as shown by the dashed curves in the foreground and the inset, respectively.

ATOMIC RESERVOIR ENGINEERING

Turning to the applications of the above-derived *ub* Hamiltonians, we next present a method to protect the Fock state $|3\rangle$, which relies on an engineered atomic reservoir [23, 24].

A bunch of atoms are required to interact with the cavity mode, one at a time, through the engineered ub Hamiltonian (7). Assuming that all the atoms are prepared in the excited state before interacting with the cavity mode under the weak coupling regime $\zeta_1\tau \ll 1$, τ being the average transit time of the atoms through the cavity, it is straightforward to obtain the master equation

$$\dot{\rho} = \frac{\Gamma}{2}\left(2A_{ub}^{\dagger}\rho A_{ub} - A_{ub}A_{ub}^{\dagger}\rho - \rho A_{ub}A_{ub}^{\dagger}\right) + \mathcal{L}\rho, \tag{10}$$

where A_{ub} is given by Eq. (8) and the effective damping rate $\Gamma = r\left(\zeta_1\tau\right)^2$, r being the arrival rate of atoms. The Lindblad form

$$\begin{aligned}\mathcal{L}\rho = &\frac{\gamma}{2}\left(1+\bar{n}\right)\left(2a\rho a^{\dagger} - \rho a^{\dagger}a - a^{\dagger}a\rho\right)\\ &+\frac{\gamma}{2}\bar{n}\left(2a^{\dagger}\rho a - \rho aa^{\dagger} - aa^{\dagger}\rho\right),\end{aligned} \tag{11}$$

describes the effect of the natural environment, at temperature $T = \hbar\omega/k_B \ln\left[\left(1+\bar{n}\right)/\bar{n}\right]$, on the cavity mode, with damping rate γ.

It is not difficult to conclude that under the condition $\Gamma \gg \gamma$, i.e., $r \gg \gamma/\left(\zeta_1\tau\right)^2$, the cavity mode —whatever its initial state— is asymptotically driven to a quasi-steady Fock state $|3\rangle$, which is the only eigenstate of $A^{\dagger}$ with null eigenvalue ($A_{ub}^{\dagger}|3\rangle = 0$). This occurs because, when $\Gamma \gg \gamma$, the engineered contribution to $\dot{\rho}$, confined to the subspace ranging from $|0\rangle$ to $|3\rangle$, prevails over the action of the thermal environment described by Eq. (11).

Assuming the same parameters as in Fig. 3(a), such that $\zeta_1 = 1.77 \times 10^3$ Hz, with $\tau = 1/r = 2 \times 10^{-4}$ s, we obtain the engineered decay rate $\Gamma = 63\gamma$, for a high-Q cavity ($\gamma \sim 10$Hz). In Fig. 4, starting with a thermal state with $\bar{n} = 0.05$, we present the evolution of the fidelity $\mathcal{F}_3(t) = \mathrm{Tr}\,|3\rangle\langle 3|\,\rho(t)$ against γt, showing that the Liouvillian (10), engineered through the ub Hamiltonian (7), leads to the steady Fock state $|3\rangle$ with fidelity around 0.92. In the inset, we plot Mandel's Q factor [25, 26], which starts from around 0.05 and goes to -0.96, indicating that the final steady state indeed approaches a Fock state.

We finally remark that, although the coupling strength of the engineered ub Hamiltonian is small in comparison with typical Rabi frequencies in microwave cavity QED, this is evidently not a limiting factor for the present proposal for the construction of stationary Fock states. Moreover, this technique to produce stationary Fock states also applies to the case of state $|2\rangle$, reached from a Liouvillian engineered from interaction (3), and state $|4\rangle$, reached from an engineered interaction confined to the Fock subspace $\{|0\rangle, |1\rangle, |2\rangle, |3\rangle, |4\rangle\}$.

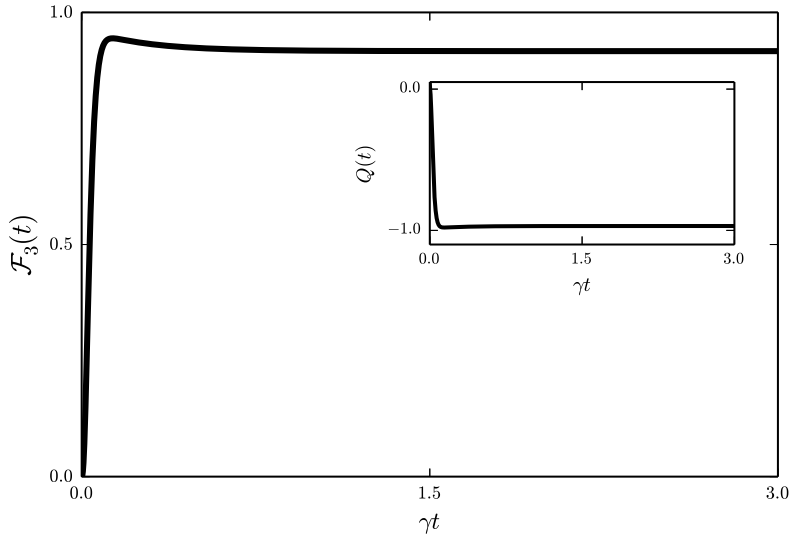

FIG. 4: Evolution of the fidelity $\mathcal{F}_3(t) = \mathrm{Tr}\,|3\rangle\langle 3|\,\rho(t)$, governed by the upper-bound Hamiltonian (3), showing that a steady Fock state $|3\rangle$ is reached with a significant fidelity, around 0.92, from a thermal state. The evolution of Mandel's Q factor is shown in the inset, indicating that the final steady state indeed approaches a Fock state.

UPPER-BOUNDED LIOUVILLIANS INDEPENDENT OF UPPER-BOUNDED HAMILTONIANS

We now present a strategy to generate *ub* Liouvillians in cavity QED which does not rely on an engineered *ub* Hamiltonian. To this end, we follow the line of reasoning in Ref. [7], where selective Liouvillians are reached by combining engineered selective Hamiltonians —governing the interaction of two-level atoms with only two Fock field states [11]— and engineered atomic reservoirs [23, 24]. For the sake of clarity, we briefly revisit the ideas developed in Ref. [7], remembering that the engineering of atomic reservoirs requires a beam of atoms to cross the cavity, interacting one at a time with the cavity mode under the weak coupling regime. Each atom must interact simultaneously with the cavity mode and a pair of laser beams, via the level configuration in Fig. 5, where an auxiliary level i is considered apart from the ground and excited states g and e. The cavity mode (ω) is used to promote a Raman-type transition $g \leftrightarrow e$, helped by the laser beams, ω_1 and ω_2, out of resonance with transitions $g \leftrightarrow i$ and $e \leftrightarrow i$, respectively. Starting with the engineering of the selective JC interactions, we write the Hamiltonian

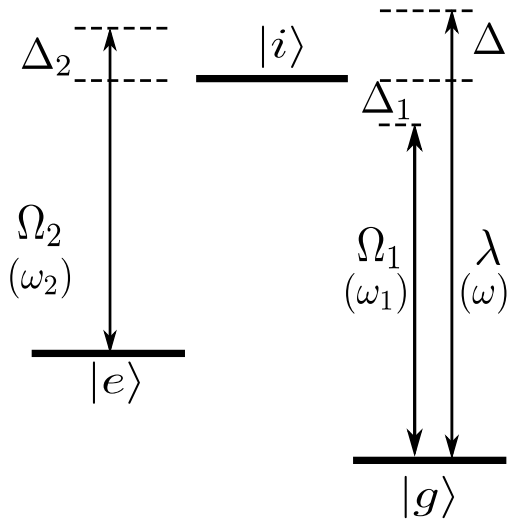

FIG. 5: Atomic level configurations to engineer selective Hamiltonians.

$$H = \lambda\sigma_{ig}a\,\mathrm{e}^{-i\Delta t} + \Omega_1\sigma_{ig}\,\mathrm{e}^{i\Delta_1 t} + \Omega_2\sigma_{ie}\,\mathrm{e}^{-i\Delta_2 t} + H.c.,$$

where $\sigma_{rs} = |r\rangle\langle s|$, r and s labelling the atomic states involved, and the detunings are defined by $\Delta = \omega - \omega_{ig}$, $\Delta_1 = \omega_{ig} - \omega_1$, and $\Delta_2 = \omega_2 - \omega_{ie}$, with $\omega_{i\ell} = \omega_i - \omega_\ell$ $(\ell = g, e)$. Under the conditions $\sqrt{\bar{n}+1}\lambda \ll \Delta$ and $\Omega_j \ll \Delta_j$ $(j = 1, 2)$, we readily derive, in the RWA, the effective interaction [21]

$$\begin{aligned} H_{eff} = &\left(\xi a^\dagger a - \varpi_g\right)\sigma_{gg} + \varpi_e\sigma_{ee} \\ &+ \left(\zeta a^\dagger\,\mathrm{e}^{i\delta t}\,\sigma_{ge} + H.c.\right), \end{aligned}$$

where $\varpi_g = |\Omega_1|^2/\Delta_1$ and $\varpi_e = |\Omega_2|^2/\Delta_2$ stand for frequency-level shifts due to the action of the classical fields, whereas the strengths $\xi = |\lambda|^2/\Delta$ and $\zeta = \lambda^*\Omega_2\left(\Delta^{-1} + \Delta_2^{-1}\right)/2$ stand respectively for off- and on-resonant atom-field couplings to be used to engineer the required selective interactions; finally, $\delta = \Delta - \Delta_2$ refers to a convenient detuning to be specified in the following lines. To get selectivity, we first perform the unitary transformation $U = \exp\left\{-i\left[\left(\xi a^\dagger a + \varpi_g\right)\sigma_{gg} + \varpi_e\sigma_{ee}\right]t\right\}$, which takes H_{eff} into the form

$$V_{eff} = \textstyle\sum_{n=1}^{\infty}\zeta_n\,|n+1\rangle\langle n|\,\sigma_{ge}\,\mathrm{e}^{i\phi_n t} + H.c..$$

with $\zeta_n = \sqrt{n+1}\zeta$ and $\phi_n = (n+1)\,\xi + \delta - \varpi_g - \varpi_e$. Next, under the strongly off-resonant regime $\xi \gg \sqrt{k+2}\,|\zeta|$ and the condition

$$\phi_k = 0,$$

which is easily satisfied by imposing $(k+1)\,\xi = \varpi_g \gg \delta = \varpi_e$, such that $|\Omega_1| = \sqrt{(k+1)\,\Delta_1/\Delta}\,|\lambda| \gg \sqrt{\Delta_1/\Delta_2}\,|\Omega_2|$, we readily eliminate, in the RWA, all the terms proportional to $\zeta_n = \sqrt{n+1}\zeta$ summed in V_{eff}, except when $n = k$, bringing about the selective interaction

$$\mathcal{H} = \left(\zeta_k \left|k+1\right\rangle \left\langle k\right| \sigma_{ge} + H.c.\right), \tag{12}$$

producing the desired selective $g \leftrightarrow e$ transition within the Fock subspace $\{\left|k\right\rangle, \left|k+1\right\rangle\}$.

Next, following the reasoning in Ref. [23, 24] for atomic reservoir engineering, it is easily shown that the Lindblad structure of the superoperator emerging from $\mathcal{H}$ does not rely on the weak-coupling regime $\zeta_k\tau \ll 1$, owing to the selective nature of this interaction. With the atoms prepared in the excited state and the subspace $\{\left|k\right\rangle, \left|k+1\right\rangle\}$ randomly selected to be $\{\left|0\right\rangle, \left|1\right\rangle\}$ and $\{\left|1\right\rangle, \left|2\right\rangle\}$, which is achieved by an appropriate adjustment of parameters, we readily obtain the selected Liouvillian (as well as from the inevitable natural Liouvillian $\mathcal{L}\rho$)

$$\dot{\rho} = \sum_{k=0}^{1} \frac{\Gamma_k}{2} \left(2\left|k+1\right\rangle \left\langle k\right| \rho \left|k\right\rangle \left\langle k+1\right| - \left|k\right\rangle \left\langle k\right| \rho - \rho \left|k\right\rangle \left\langle k\right|\right) + \mathcal{L}\rho, \tag{13}$$

with $\Gamma_k = r(\zeta_k\tau)^2$, which is somewhat different from that in Eq. (10). In fact, the above equation does not contain the crossed terms coupling together the two selected subspaces $\{\left|0\right\rangle, \left|1\right\rangle\}$ and $\{\left|1\right\rangle, \left|2\right\rangle\}$, that naturally arise in Eq. (10). Evidently, we can build other ub Liouvillians by selecting additional subspaces beyond those arising from $k = 0$ and $k = 1$. As a final remark, before applying the engineered Liouvillian (13) to produce steady Fock states, we observe that this Liouvillian does not emerge from an ub Hamiltonian, as did the previous one given by Eq. (10). Its derivation relies, instead, on the engineered selective interactions given by Eq. (12).

To estimate the range of validity of the parameters leading to Hamiltonian (12), we start by choosing $\Delta = \Delta_1 = (1 + 10^{-2}) \times \Delta_2 = 10\sqrt{k+1}\,|\lambda|$, such that $|\Omega_1| = 10 \times |\Omega_2| = \sqrt{k+1}\,|\lambda|$, $\zeta_k = 10^{-2}\sqrt{k+1}\,|\lambda|$, and $\tau = 1/r = 10^2/\sqrt{\max(k)+1}\,|\lambda|$, so that $\zeta_{\max(k)}\tau = 1$, and $\Gamma_k = \left\{(k+1)\,|\lambda| \,/\, [\max(k)+1]^{3/2}\right\} \times 10^{-2}$. Assuming typical $\lambda \sim 5 \times 10^5$Hz, $\gamma \sim 10$Hz [22] and $\bar{n} = 0.05$, in Fig. 6(a), we plot the evolution of the fidelity $\mathcal{F}_2(t) = \mathrm{Tr}\left|2\right\rangle \left\langle 2\right| \rho(t)$ against γt, setting $\tau = 1/r = \sqrt{2} \times 10^{-4}$s, $\Gamma_0 = 176\gamma$ and $\Gamma_1 = 2\Gamma_0$. We obtain a fidelity around 0.95. Using the same typical parameters, in Fig. 6(b) we display the evolution of

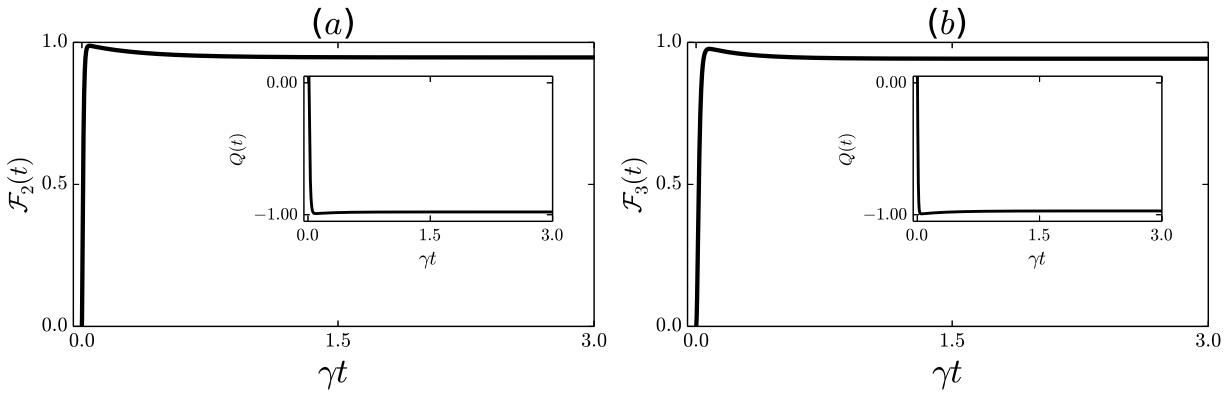

FIG. 6: (a) Evolution of the fidelity $\mathcal{F}_2(t) = \mathrm{Tr}\,|2\rangle\langle 2|\,\rho(t)$, governed by Eq. (13), showing that a steady Fock state $|2\rangle$ is reached with a significant fidelity, around 0.95, from a thermal state. The evolution of Mandel's Q factor, shown in the inset, leads to a value around -0.98, indicating that the final steady state indeed approaches a Fock state. (b) Evolution of the fidelity $\mathcal{F}_3(t) = \mathrm{Tr}\,|3\rangle\langle 3|\,\rho(t)$, governed by Eq. (13), showing that a steady Fock state $|3\rangle$ is reached with a significant fidelity, around 0.94, from a thermal state. The evolution of Mandel's Q factor, shown in the inset, leads to a value around -0.97, indicating that the final steady state indeed approaches a Fock state.

the fidelity $\mathcal{F}_3(t)$ against γt, with $\tau = 1/r = 2 \times 10^{-4}/\sqrt{3}$s, $\Gamma_0 = 96\gamma$, $\Gamma_1 = 2\Gamma_0$, and $\Gamma_2 = 3\Gamma_0$, reaching a fidelity around 0.94. In the inset in Figs. 6(a and b), we plot Mandel's Q factor, which tends to -0.98 and -0.97, respectively, showing that we indeed approach a Fock state in both cases.

CONCLUSIONS

We have thus presented a technique to engineer *ub* and sliced atom-field interactions in cavity QED. We started by engineering these interactions confined to the Fock subspaces $\{|0\rangle, |1\rangle, |2\rangle\}$ and $\{|M\rangle, |M+1\rangle, |M+2\rangle\}$, respectively, using a four-level atomic configuration, a cavity mode and a laser field. Next, with the same cavity mode and laser field but with a five-level atomic configuration, we showed how to engineer interactions confined to the Fock subspaces ranging from $|0\rangle$ to $|3\rangle$ and $|M\rangle$ to $|M+3\rangle$. The validity of these engineered interactions was confirmed by comparing the evolution of the cavity mode population described by them with those described by the full Hamiltonians from which they were derived. All the numerical simulations in this work were performed using QuTIP [27]. We

have also indicated how to generate, through a six-level atomic configuration, interactions confined to the Fock subspaces ranging from $|0\rangle$ to $|3\rangle$ and $|M\rangle$ to $|M+4\rangle$.

Next, turning to the applications of the derived *ub* Hamiltonians confined to a subspace of states ranging from $|0\rangle$ up to $|N\rangle$, we presented a method, relying on atomic reservoir engineering [23, 24], for the protection of the higher energy state $|N\rangle$. Focusing on the *ub* Hamiltonian confined to the Fock subspaces $\{|0\rangle, |1\rangle, |2\rangle, |3\rangle\}$, we presented the evolution of the fidelity $\mathcal{F}_3(t) = \mathrm{Tr}\,|3\rangle\langle 3|\,\rho(t)$ and Mandel's Q factor, showing that the field reaches the steady state that indeed approaches the Fock state $|3\rangle$.

We then present a strategy —following the reasoning in Ref. [7], where engineered atomic reservoirs [23, 24] are also assumed— to generate *ub* Liouvillians, which does not rely on the engineering of a specific *ub* Hamiltonian. The engineered Liouvillian is then used to generate and protect states that approach closely the Fock states $|2\rangle$ and $|3\rangle$.

The two schemes outlined above for the production of steady Fock states have approximately the same effectiveness and difficulty of practical implementation. The engineering of *ub* Hamiltonians and Liouvillians becomes increasingly difficult as we increase the size of the *ub* subspace. While the engineering of *ub* interactions requires an increasing number of specific atomic levels and laser beams, the engineering of *ub* Liouvillians demands the random selection of an increasing number of the subspaces $\{|k\rangle, |k+1\rangle\}$.

We finally observe that a number of distinct applications of the *ub* and sliced interactions we have engineered above can be implemented, such as the engineering of non-classical states, quantum logical gates, teleportation of superpositions of $N > 2$, etc. Basically, what we have done in this contribution can be taken forward in the context of what have been called quantum-scissors for optical state truncation [12]. As already stressed above, the technique here presented can be directly applicable, among others platforms, to circuit QED [9].

Acknowledgements

The authors acknowledge financial support from PRP/USP within the Research Support Center Initiative (NAP Q-NANO) and FAPESP, CNPQ and CAPES, Brazilian agencies.

[1] J. I. Cirac, and P. Zoller, Phys. Rev. Lett. **74**, 4091 (1995).

[2] S.-B. Zheng and G.-C. Guo, Phys. Rev. Lett. **85**, 2392 (2000).

[3] R. M. Serra, C. J. Villas-Bôas, N. G. de Almeida, and M. H. Y. Moussa, Phys. Rev. A **71**, 045802 (2005); *ibid.* Phys. Rev. A 71, 045802 (2005); C. J. Villas-Bôas and M. H. Y. Moussa, Eur. Phys. J. D **32**, 147 (2005).

[4] R. Gerritsma *et al.*, Nature **463**, 68 (2010); L. Lamata *et al.*, Phys. Rev. Lett. **98**, 253005 (2007); C. Monroe *et al.*, Science **272**, 1131 (1995); Q. A. Turchette *et al.*, Phys. Rev. Lett. **81**, 3631 (1998); C. J. Myatt *et al.*, Nature **403**, 269 (2000); M. A. Rowe et al., Nature **409**, 791 (2001); M. D. Barrett *et al.*, Nature **429** (2004); D. Leibfried *et al.*, Nature **438**, 639 (2005); D. J. Wineland, Rev. Mod. Phys. **75**, 4714 (2013); C. Monroe *et al.*, Phys. Rev. Lett. **75**, 4714 (1995); D. Kielpinski *et al.*, Nature **417**, 709 (2002); J. Chiaverini *et al.*, Nature 432, 602 (2004); J. P. Home *et al.*, Science **325**, 1227 (2009); C. Ospelkaus *et al.*, Nature 476, 181 (2011); J. P. Gaebler, *et al.*, Phys. Rev. Lett. **109**, 179902 (2012); A. Bermudez *et al.*, Phys. Rev. A **76**, 041801(R) (2007); Schliemann *et al.*, Phys. Rev. Lett. **94**, 266801 (2005); X. Zhang, Phys. Rev. Lett. **100**, 113903 (2008); J. Y. Vaishnaw *et al.*, Phys. Rev. Lett. **100**, 153002 (2008); L. J. Garay *et al.*, Phys. Rev. Lett. **85**, 4643 (2000).

[5] J. F. Poyatos, J. I. Cirac, and P. Zoller, Phys. Rev. Lett. **77**, 4728 (1996); F. O. Prado, E. I. Duzzioni, M. H. Y. Moussa, N. G. de Almeida, and C. J. Villas-Bôas, Phys. Rev. Lett. **102**, 073008 (2009);

[6] L. C. Celeri, M. A. de Ponte, C. J. Villas-Boas, and M H Y Moussa, J. Phys. B: At. Mol. Opt. Phys. **41,** 085504 (2008).

[7] F. O. Prado, W. Rosado, G. D. de Moraes Neto and M. H. Y. Moussa, EPL **107,** 13001 (2014).

[8] R. F. Rossetti, G. D. de Moraes Neto, F. O. Prado, F. Brito, and M. H. Y. Moussa, Phys. Rev. A **90**, 033840 (2014).

[9] G. Zhu, D. G. Ferguson, V. E. Manucharyan, and J. Koch, Phys. Rev. B **87**, 024510 (2013).

[10] G. D. de Moraes Neto, W. Rosado, F. O. Prado, and M. H. Y. Moussa, arXiv:1409.6783.

[11] F. O. Prado, W. Rosado, A. M. Alcalde, and M. H. Y. Moussa, J. Phys. B: At. Mol. Opt. Phys. **46**, 205501 (2013).

[12] D. T. Pegg, L. S. Phillips, and S. M. Barnett, Phys. Rev. Lett. **81**, 1604 (1998); Ş. K. Özdemir, A. Miranowicz, M. Koashi, and N. Imoto, Phys. Rev. A **64**, 063818 (2001); W. Leoński and A. Kowalewska-Kudłaszyk, Progress in Optics **56**, 131-185 (2011).

[13] Z. Kis, W. Vogel, and L. Davidovich, Phys. Rev. A **64**, 033401 (2001).

[14] S. Diehl, A. Micheli, A. Kantian, B. Kraus, H. P. Buchler, and P. Zoller, Nature phys. **4**, 878 (2008); B. Kraus, H. P. Büchler, S. Diehl, A. Kantian, A. Micheli, and P. Zoller1, Phys. Rev. A **78**, 042307 (2008); M. Müller, S. Diehl, G. Pupillo, P. Zoller, Adv. At. Mol. Opt. Phys. **61**, 1 (2012).

[15] Z. Leghtas, U. Vool, S. Shankar, M. Hatridge, S. M. Girvin, M. H. Devoret, and M. Mirrahimi, Phys. Rev. A **88**, 023849 (2013).

[16] F. Ticozzi and L. Viola, Quantum Inf. Comput. **14**, 0265 (2014).

[17] B. T. H. Varcoe, S. Brattke, M. Weidinger, and H. Walther, Nature **403**, 743 (2000); P. Bertet, S. Osnaghi, P. Milman, A. Auffeves, P. Maioli, M. Brune, J. M. Raimond, and S. Haroche, Phys. Rev. Lett. **88**, 143601 (2002).

[18] D. M. Meekhof, C. Monroe, B. E. King, W. M. Itano, and D. J. Wineland, Phys. Rev. Lett. **76**, 1796 (1996); D. Leibfried, D. M. Meekhof, B. E. King, C. Monroe, W. M. Itano, and D. J. Wineland, Phys. Rev. Lett. **77**, 4281 (1996).

[19] M. Hofheinz, E. M. Weig, M. Ansmann, R. C. Bialczak1, E. Lucero, M. Neeley, A. D. O'Connell, H. Wang, J. M. Martinis, and A. N. Cleland, Nature **454**, 310 (2008).

[20] X. Zhou, I. Dotsenko, B. Peaudecerf, T. Rybarczyk, C. Sayrin, S. Gleyzes, J. M. Raimond, M. Brune, and S. Haroche, Phys. Rev. Lett. **108**, 243602 (2012).

[21] O. Gamel and D. F. V. James, Phys. Rev. A **82**, 052106 (2010); D. F. V. James and J. Jerke, Can. J. Phys. **85**, 625 (2007).

[22] J. M. Raimond, M. Brune, and S. Haroche, Rev. Mod. Phys. **73**, 565 (2001).

[23] B.-G. Englert and G. Morigi, in Coherent Evolution in Noisy Environments, edited by A. Buchleitner and K. Hornberger (Springer, Berlin, 2002), p. 55.

[24] S. Pielawa, G. Morigi, D. Vitali, and L. Davidovich, Phys. Rev. Lett. 98, 240401 (2007); S. Pielawa, L. Davidovich, D. Vitali, and G. Morigi, Phys. Rev. A **81**, 043802 (2010); S. Pielawa, G. Morigi, D. Vitali, and L. Davidovich, Phys. Rev. A **85**, 022120 (2012).

[25] D. F. Walls and G. J. Milburn, *Quantum Optics* (Springer-Verlag, Berlin, 1995).

[26] M. O. Scully and M. S. Zubairy, *Quantum Optics* (Cambridge University Press, 1997)

[27] J. R. Johansson, P. D. Nation, and F. Nori, Comput. Phys. Commun. **183**, 1760 (2012); *ibid.* **184**, 1234 (2013).